ChemPubSoc Europe

DOI: 10.1002/chem.201705388

CHEMISTRY A European Journal Full Paper

Ruthenium Complexes |*Hot Paper*|

Effects of the Bidentate Ligand on the Photophysical Properties, Cellular Uptake, and (Photo)cytotoxicity of Glycoconjugates Based on the $[Ru(tpy)(NN)(L)]^{2+}$ Scaffold

Lucien N. Lameijer,[a] Tobias G. Brevé,[a] Vincent H. S. van Rixel,[a] Sven H. C. Askes,[a] M. A. Siegler,[b] and Sylvestre Bonnet*[a]

Abstract: Ruthenium polypyridyl complexes have received widespread attention as potential chemotherapeutics in photodynamic therapy (PDT) and in photochemotherapy (PACT). Here, we investigate a series of sixteen ruthenium polypyridyl complexes with general formula $[Ru(tpy)(N–N)(L)]^{+/2+}$ (tpy = 2,2′:6′,2″-terpyridine, N–N = bpy (2,2′-bipyridine), phen (1,10-phenanthroline), dpq (pyrazino[2,3-*f*][1,10]phenanthroline), dppz (dipyrido[3,2-*a*:2′,3′-*c*]phenazine, dppn (benzo[*i*]dipyrido[3,2-*a*:2′,3′-*c*]phenazine), pmip (2-(4-methylphenyl)-1*H*-imidazo[4,5-*f*][1,10]phenanthroline), pymi ((*E*)-*N*-phenyl-1-(pyridin-2-yl)methanimine), or azpy (2-(phenylazo)pyridine), L = Cl^- or 2-(2-(2-(methylthio)ethoxy)ethoxy)ethyl-β-d-glucopyranoside) and their potential for either PDT or PACT. We demonstrate that although increased lipophilicity is generally related to increased uptake of these complexes, it does not necessarily lead to increased (photo)cytotoxicity. However, the non-toxic complexes are excellent candidates as PACT carriers.

Introduction

Ruthenium based anti-cancer compounds have been investigated for several decades[1] as potential alternatives to the clinically approved cisplatin. Cisplatin is associated with serious side effects such as renal toxicity, neurotoxicity, and hearing loss.[2] The most thoroughly investigated ruthenium-based anti-cancer agents, NAMI-A and KP1019, both reached phase II clinical trials before being abandoned.[3] More recently, the tunable photophysical properties of ruthenium(II) polypyridyl complexes have been used to develop compounds combating bacterial resistance to antibiotics,[4] or new photosensitizers for photodynamic therapy as an alternative to, for example, Photofrin.[5] Recently, the group of McFarland have made a great step forward in this field, by entering phase I clinical trials with a Ru^{II}-thiophene-polypyridyl-based photosensitizer, TLD1433.[6] Simultaneously, a great interest has been shown in the development of sterically strained ruthenium(II) complexes for the light-induced delivery of cytotoxic cargo.[7] This last approach is often referred to as photo-activated chemotherapy (PACT).[3b,8] The proof-of-concept for ruthenium-based PACT was first demonstrated by Etchenique's group, who demonstrated the photorelease of the potassium channel blocker 4-aminopyridine (4AP) from $[Ru(bpy)_2(4AP)_2]^{2+}$ upon visible light irradiation.[9] Many other examples of ruthenium complexes used as photosensitive agents releasing anticancer molecules have been developed by the group of Turro,[10] Gasser,[11] Glazer,[12] Kodanko,[13] and Bonnet.[14] Following up on our initial work using thioether monodentate ligands to cage cytotoxic aqua ruthenium complexes,[14b,15] we report here a series of related chloride complexes [**1 a**]Cl–[**8 a**]Cl having the general formula [Ru(tpy)(N–N)(Cl)]Cl with N–N = bpy (2,2′-bipyridine), phen (1,10-phenanthroline), dpq (pyrazino[2,3-*f*][1,10]phenanthroline), dppz (dipyrido[3,2-*a*:2′,3′-*c*]phenazine, dppn (benzo[*i*]dipyrido[3,2-*a*:2′,3′-*c*]phenazine), pmip (2-(4-methylphenyl)-1*H*-imidazo[4,5-*f*][1,10]phenanthroline), pymi ((*E*)-*N*-phenyl-1-(pyridin-2-yl)methanimine), or azpy (2-(phenylazo)pyridine), and of their water-soluble derivatives $[Ru(tpy)(N–N)(\mathbf{R})](PF_6)_2$ ($[\mathbf{1\,b}](PF_6)_2$–$[\mathbf{8\,b}](PF_6)_2$), in which **R** = (2-(2-(2-(methylthio)ethoxy)ethoxy)ethyl-β-d-glucopyranoside is a thioether-glucose conjugate (Figure 1).

On the one hand, [Ru(tpy)(bpy)(Cl)]Cl is known to be poorly cytotoxic to cancer cells.[1d] On the other hand, we recently demonstrated that $[Ru(tpy)(dppn)(\mathbf{R})](PF_6)_2$ ($[\mathbf{5\,b}](PF_6)_2$, (Figure 1) has unique phototoxic properties based on a dual mode-of-action involving both photosubstitution of the thioether ligand and singlet oxygen generation. In this paper, we compare the photophysical properties of all conjugates $[\mathbf{1\,b}](PF_6)_2$–$[\mathbf{8\,b}](PF_6)_2$ and of their chloride analogues [**1 a**]Cl–

[a] *L. N. Lameijer, T. G. Brevé, Dr. V. H. S. van Rixel, S. H. C. Askes, Dr. S. Bonnet*
Leiden Institute of Chemistry, Leiden University
Gorlaeus Laboratories, P.O. Box 9502, 2300 RA Leiden (The Netherlands)
E-mail: bonnet@chem.leidenuniv.nl

[b] *Dr. M. A. Siegler*
Departement of Chemistry, Johns Hopkins University
Baltimore, Maryland 21218 (USA)

Supporting information and the ORCID number(s) for the author(s) of this article can be found under https://doi.org/10.1002/chem.201705388.

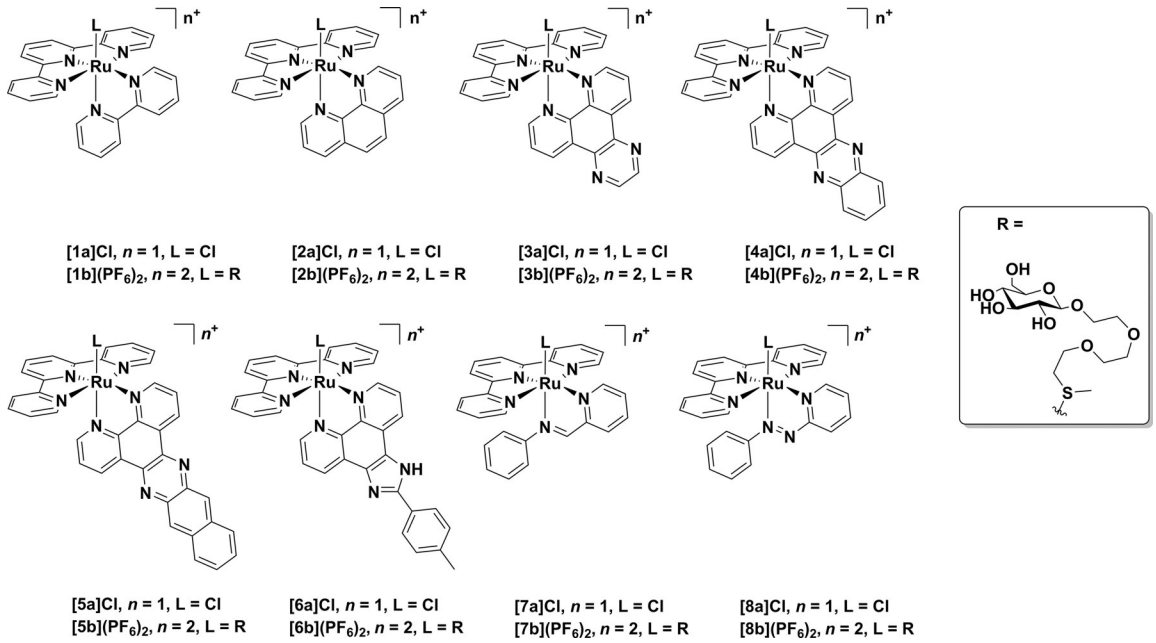

Figure 1. Chemical structure of the complexes used in this study. General formula $[Ru(tpy)(N{-}N)(\mathbf{R})]^{n+}$, N–N = bpy, phen, dpq, dppz, dppn, pmip, pymi or azpy. L = Cl^- or L = **R** (2-(2-(2-(methylthio)ethoxy)ethoxy)ethyl-β-d-glucopyranoside).

[**8a**]Cl in water, and correlate them to the uptake and cytotoxicity in cancer cells. Critically, the glucose-containing ligand L ensures that all thioether-ruthenium complexes are soluble in water, allowing their photochemistry to be studied independently from the lipophilicity of the N–N spectator bidentate ligand.

Results

Synthesis

Chloride complexes [**1a**]Cl,[16] [**2a**]Cl,[17] [**4a**]Cl,[18] [**5a**]Cl,[14b] [**7a**]Cl,[19] [**8a**]Cl,[20] and the ligand 2-(2-(2-(methylthio)ethoxy)-ethoxy)ethyl-β-d-glucopyranoside (**R**)[14b] were synthesized as reported previously. Complexes [**3a**]Cl and [**6a**]Cl were synthesized by reacting $[Ru(tpy)Cl_3]$ with the bidentate ligand dpq or pmip in the presence of triethylamine as a reducing agent. The chloride complexes [**1a**]Cl–[**8a**]Cl were then reacted with an excess of the thioether ligand **R** in the dark in water. Silica column purification of the crude complexes, followed by size exclusion chromatography, afforded the thioether-glucose ruthenium conjugates [**1b**]$(PF_6)_2$, [**2b**]$(PF_6)_2$ and [**4b**]$(PF_6)_2$ as orange to red solids and [**8b**]$(PF_6)_2$ as a purple solid. To ease purification of the pmip complex [**6b**]$(PF_6)_2$, the synthesis was carried out similarly to the previously reported synthesis of [**5b**]$(PF_6)_2$[14b] by first converting the chloride precursor [**5a**]Cl to the aqua species $[Ru(tpy)(pmip)(H_2O)](PF_6)_2$ using $AgNO_3$ and NH_4PF_6 followed by reaction of the thioether ligand with the aqua complex. Similarly, the syntheses of [**3b**]$(PF_6)_2$ and [**7b**]$(PF_6)_2$ were carried out in the presence of $AgPF_6$ to ensure in situ conversion of the chlorido precursor into the aqua species before coordination of the thioether ligand. All chloride complexes except [**4a**]Cl, [**5a**]Cl and [**6a**]Cl and all thioether complexes are soluble in water. As reported for the complex $[Ru(tpy)(bpy)(Hmte)](PF_6)_2$,[21] all thioether complexes showed an upfield shift of the methylsulfide group to about 1.5 ppm in the ^1H NMR spectra, confirming coordination of the thioether donor atom to the ruthenium center. All new compounds were characterized using NMR spectroscopy, thin layer chromatography, electronic absorption spectroscopy, high-resolution mass spectrometry, and elemental analysis.

Crystal structures

Attempts to crystallize the glycoconjugates [**1b**]$(PF_6)_2$–[**8b**]$(PF_6)_2$ were unsuccessful and usually led to the formation of oils or colloidal suspensions. However, single crystals suitable for X-ray diffraction analyses were obtained for [**5a**]Cl, and for [**3a**]PF_6 and [**4a**]PF_6 after salt metathesis of [**3a**]Cl and [**4a**]Cl using aqueous NH_4PF_6, followed by vapor diffusion of diethyl ether in a solution of [**3a**]PF_6 in acetone or acetone in a solution of [**4a**]PF_6 in ethyl acetate (Figure 2). The three crystal structures showed the expected distorted octahedral geometry, with a reduced (< 180°) N-Ru-N angle for the coordinated terpyridine ligand (N1-Ru1-N3, 159.11–159.40°, Table 1). The bidentate ligands dpq, dppz and dppn are all bound perpendicular to tpy, with a N4-Ru1-N5 bite angle of 79.26–80.2° (Table 1). The Ru1–Cl1 bond lengths were found to be similar with values ranging from 2.4015 to 2.4165 Å which are very close to reported values for related complexes.[22] Selected bond lengths and angles are given in Table 1.

Photophysical properties of the $[Ru(tpy)(NN)(L)]^{n+}$ complexes

The photophysical properties of chloride complexes [**1a**]Cl–[**8a**]Cl were first investigated in acetonitrile, in which the com-

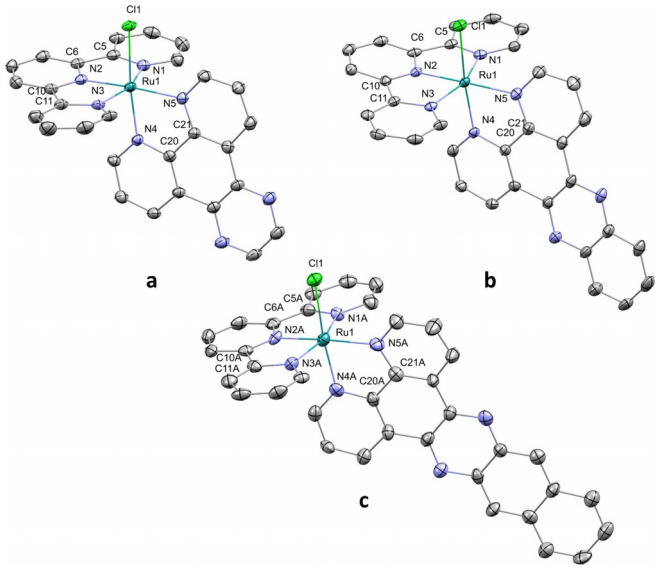

Figure 2. Displacement ellipsoid plots (50% probability level) of the complex cation [**3a**]PF_6, [**4a**]PF_6.$(CH_3)_2CO$ and [**5a**]Cl at 110(2) K. For [**5a**]Cl only one of the independent molecules is shown. Hydrogen atoms, counter-ions, and lattice solvent molecules, have been omitted for clarity.

Table 1. Selected bond lengths [Å] and bond angles [°] for complexes [**3a**]PF_6, [**4a**]PF_6.$(CH_3)_2CO$ and [**5a**]Cl.

	[**3a**]$(PF_6)_2$	[**4a**]$(PF_6)_2$	[**5a**]Cl[a]
Ru1–Cl1	2.4062(5)	2.4015(7)	2.4165(17)
Ru1–N1	2.069(2)	2.053(2)	2.048(5)
Ru1–N2	1.9569(19)	1.957(2)	1.953(5)
Ru1–N3	2.058(2)	2.064(2)	2.050(5)
Ru1–N4	2.046(2)	2.044(2)	2.043(5)
Ru1–N5	2.0917(19)	2.074(2)	2.073(5)
C5–C6	1.472(3)	1.469(4)	1.469(9)
C5–N1	1.369(3)	1.372(3)	1.389(8)
C6–N2	1.355(3)	1.357(3)	1.340(7)
C10–C11	1.478(3)	1.479(4)	1.484(8)
C10–N2	1.355(3)	1.349(4)	1.340(7)
C11–N3	1.371(3)	1.372(3)	1.384(7)
C20–C21	1.446(3)	1.440(4)	1.459(8)
C20–N4	1.370(3)	1.371(3)	1.370(7)
C21–N5	1.364(3)	1.362(3)	1.379(8)
N1-Ru1-N3	159.10(8)	159.58(9)	159.67(19)
N4-Ru1-N5	79.45(8)	79.26(9)	80.2(2)

[a] Values for Ru1Å.

plexes are all soluble and do not hydrolyze. The chloride complexes [**1a**]Cl–[**8a**]Cl show a ^{1}MLCT bands varying between 501 and 523 nm, with molar absorptivities ranging from 9.1×10^3 to $12.8\times10^3\,M^{-1}\,cm^{-1}$ (Table 2), comparable to reported values for ruthenium(II) polypyridyl complexes.[7,12,15c,23] All complexes have very low phosphorescence quantum yields ($\Phi_p<10^{-4}$) except for [**2a**]Cl, [**5a**]Cl, and [**6a**]Cl that are weakly emissive ($\Phi_p=10^{-3}$ to 10^{-4}). The $^1O_2$ generation quantum yield in CD_3OD are low ($\Phi_\Delta\leq0.05$), with the exception of [**6a**]Cl ($\Phi_\Delta=8.2\times10^{-2}$), which is also the most emissive complex.

The hydrophilicity of the thioether analogues [**1b**]$(PF_6)_2$–[**8b**]$(PF_6)_2$ allowed for studying photosubstitution quantum yields in MilliQ water using electronic absorption spectroscopy. Monochromatic blue light (450 or 470 nm) was used to irradiate the complexes in their ^{1}MLCT absorption band. Although all thioether complexes are thermally stable at room temperature, seven of the eight complexes, that is, [**1b**]$(PF_6)_2$ to [**7b**]$(PF_6)_2$, showed light-induced exchange of their thioether ligand for H_2O.

The ligand photosubstitution was characterized by clear isosbestic points in the UV/Vis spectra (450 to 476 nm depending on the compound), as shown in Figure 3. For each of these reactions a bathochromic shift of the ^{1}MLCT band was observed,

Table 2. Lowest-energy absorption maxima [λ_{max}], molar absorption coefficients at λ_{max} [ε_{max} in $M^{-1}\,cm^{-1}$] and λ_{450} [ε_{450} in $M^{-1}\,cm^{-1}$], photosubstitution quantum yields [Φ_{450}] at 298 K, $^1O_2$ quantum yields [Φ_Δ] at 293 K, photosubstitution reactivity [$\xi=\Phi_{450}\,x\,\varepsilon_{450}$], and phosphorescence quantum yield [Φ_P] at 293 K for complexes [**1a**]Cl–[**8a**]C and, [**1b**]$(PF_6)_2$–[**8b**]$(PF_6)_2$.

Complex	λ_{max} [nm] (ε_{max} [$M^{-1}\,cm^{-1}$])[a]	ε_{450} [$M^{-1}\,cm^{-1}$]	Φ_{450}[b]	ξ	Φ_Δ[c]	Φ_p[c]
[**1a**]Cl	504 (9.1×10^3)	4.6×10^3	–	–	0.055	$<1\times10^{-5}$
[**2a**]Cl	501 (9.1×10^3)	6.5×10^3	–	–	0.048	8.5×10^{-4}
[**3a**]Cl	504 (9.1×10^3)	6.6×10^3	–	–	0.055	$<1\times10^{-5}$
[**4a**]Cl	511 (9.6×10^3)	5.6×10^3	–	–	0.005	$<1\times10^{-5}$
[**5a**]Cl	498 (12.0×10^3)	8.5×10^3	–	–	0.023	4.3×10^{-4}
[**6a**]Cl	501 (1.12×10^3)	6.8×10^3	–	–	0.082	3.2×10^{-3}
[**7a**]Cl	523 (13.0×10^3)	3.4×10^3	–	–	0.012	1.4×10^{-5}
[**8a**]Cl	508 (12.2×10^3)	3.9×10^3	–	–	<0.001	1.8×10^{-5}
[**1b**]$(PF_6)_2$	450 (7.0×10^3)	7.0×10^3	0.0084	59	0.020 (0.020)	$<1\times10^{-5}$
[**2b**]$(PF_6)_2$	448 (6.2×10^3)	6.2×10^3	0.0065	40	0.050 (0.080)	1.2×10^{-4}
[**3b**]$(PF_6)_2$	448 (8.9×10^3)	8.9×10^3	0.0067	60	0.030 (0.010)	$<1\times10^{-5}$
[**4b**]$(PF_6)_2$	458 (13.1×10^3)	12.8×10^3	0.020	256	0.0010 (0.0030)	$<1\times10^{-5}$
[**5b**]$(PF_6)_2$	458 (11.6×10^3)	11.4×10^3	0.00095	11	0.71/(0.41)	$<1\times10^{-5}$
[**6b**]$(PF_6)_2$	460 (11.0×10^3)	10.4×10^3	0.0070	73	0.0020	$<1\times10^{-5}$
[**7b**]$(PF_6)_2$	472 (11.7×10^3)	11.7×10^3	0.0053	62	0. 11 (0.14)	2.5×10^{-3}
[**8b**]$(PF_6)_2$	505 (7.2×10^3)	2.7×10^3	-	-	0.0070(–)	$<1\times10^{-5}$

[a In MeCN for [**1a**]Cl–[**8a**]Cl and in MilliQ H_2O for [**1b**]$(PF_6)_2$–[**8b**]$(PF_6)_2$. [b] in H_2O. $\lambda_{irr}=450$ nm for [**1b**]$(PF_6)_2$–[**6b**]$(PF_6)_2$ and 470 nm for [**7b**]$(PF_6)_2$. [c] in CD_3OD.

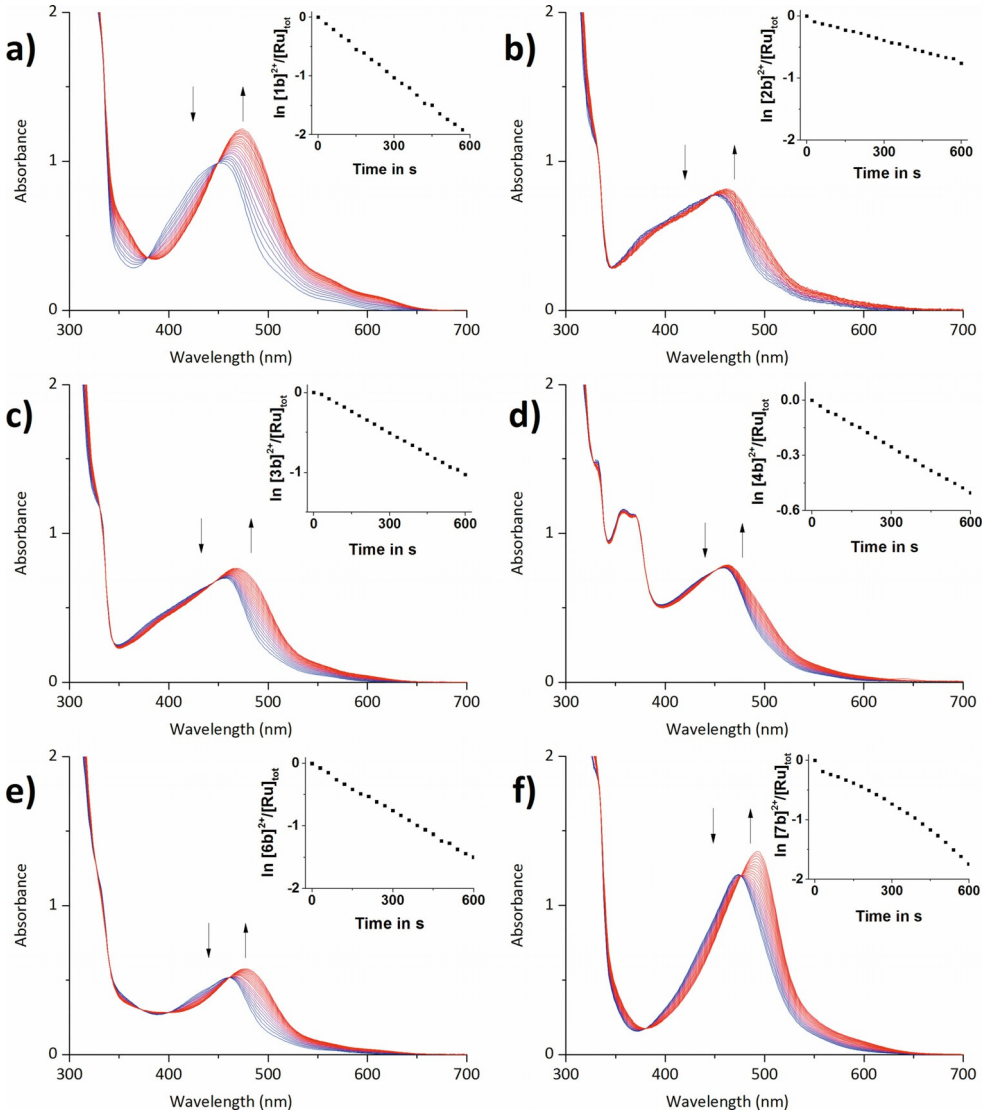

Figure 3. Electronic absorption spectra of [**1 b**]$(PF_6)_2$–[**4 b**]$(PF_6)_2$, [**6 b**]$(PF_6)_2$ and [**7 b**]$(PF_6)_2$ in deoxygenated H_2O upon irradiation at 450 or 470 nm for 5 min at $T = 298$ K. Spectra measured every 30 s. a) [**1 b**]$(PF_6)_2$, $[Ru]_{tot} = 1.38\times10^{-4}$ M, $\lambda_{exc} = 450$ nm, photon flux $= 1.71\times10^{-7}$ mol s^{-1}. b) [**2 b**]$(PF_6)_2$, $[Ru]_{tot} = 1.15\times10^{-4}$ M, $\lambda_{exc} = 450$ nm, photon flux $= 6.83\times10^{-8}$ mol s^{-1}. c) [**3 b**]$(PF_6)_2$, $[Ru]_{tot} = 7.91\times10^{-5}$ M, $\lambda_{exc} = 450$ nm, photon flux $= 5.29\times10^{-8}$ mol s^{-1}. d) [**4 b**]$(PF_6)_2$, $[Ru]_{tot} = 8.66\times10^{-5}$ M, $\lambda_{exc} = 450$ nm, photon flux $= 2.84\times10^{-8}$ mol s^{-1}. e) [**6 b**]$(PF_6)_2$, $[Ru]_{tot} = 4.75\times10^{-5}$ M, $\lambda_{exc} = 450$ nm, photon flux $= 4.97\times10^{-8}$ mol s^{-1}. f) [**7 b**]$(PF_6)_2$, $[Ru]_{tot} = 8.88\times10^{-5}$ M, $\lambda_{exc} = 470$ nm, photon flux $= 1.52\times10^{-7}$ mol s^{-1}. Inset depicts the evolution of ln $[Ru]_{SRR'}/[Ru]_{tot}$ vs. irradiation time in s, in which $[Ru]_{SRR'}$ represents the concentration of ruthenium-thioether complex at time t, and $[Ru]_{tot}$ the total ruthenium concentration.

which is consistent with earlier reports on the formation of monoaqua-ruthenium complexes in aqueous solution.[15a] Most complexes have a photosubstitution quantum yield (Φ_{450}) of 0.5–2 percent, leading to photosubstitution reactivities ($\xi = \Phi_{450} < mx > \varepsilon_{450}$, in which ε_{450} is the molar absorption at 450 nm) on the order of ten to hundreds ($\xi = 11$–256). Changing the bidentate ligand has thus a significant influence on the photosubstitution rates. Interestingly, the dppz complex [**4 b**]$^{2+}$ has the highest photosubstitution quantum yield of the series, which is also about 20-fold higher ($\Phi_{450} = 0.020$) than that of the structurally similar dppn analogue [**5 b**]$^{2+}$, which showed the lowest Φ_{450} (0.00095).[14b] Furthermore, [**4 b**]$^{2+}$ produces minimal amounts of $^1O_2$ ($\Phi_\Delta = 0.0010$) and is poorly emissive ($\Phi_P = < 1\times10^{-5}$), which indicates that contrary to the dppn complex [**5 b**]$^{2+}$ for which light irradiation leads to low-lying $^3\pi\pi^*$ excited states located on the spectator bidentate ligand,[14b] with the dppz complex such $^3\pi\pi^*$ states are either too high in energy to be populated, or outcompeted by a rather quick conversion to the photodissociative metal-centered triplet state (^{3}MC).

Another interesting observation concerned the difference in reactivity between [**7 b**]$^{2+}$ and [**8 b**]$^{2+}$. Whereas [**7 b**]$^{2+}$ displayed ligand dissociation efficiency comparable to that of the bpy complex [**1 b**]$^{2+}$, the azpy compound [**8 b**]$^{2+}$ did not show any ligand photosubstitution, indicating a strong electronic effect of the azo ligand on the photoreactivity of its ruthenium complex. The ^{1}MLCT absorption maximum for [**8 b**]$^{2+}$ is significantly lower in energy (505 nm) than that of [**7 b**]$^{2+}$ (472 nm), which points to the low energy of the azo-based π^* orbital of the azpy ligand, leading to a low-lying ^{3}MLCT state for the

complex. Considering that there is no steric strain in this complex to lower the ^{3}MC state,[23b] the ^{3}MC-^{3}MLCT energy gap is very large in $[\mathbf{8b}]^{2+}$, therefore preventing photosubstitution reactions to occur. It should be noted that $[\mathbf{8b}]^{2+}$ is not emissive at all ($\Phi_P < 1\times10^{-5}$) and has a negligible $^1O_2$ generation quantum yield (0.007), and thus that non-radiative decay is the main deactivation pathway for this complex. Regarding singlet oxygen generation, most of the other complexes produced small amounts of $^1O_2$ in CD_3OD ($\Phi_\Delta = 0.002$–0.14), with the exception of $[\mathbf{5b}]^{2+}$ that has a very high $^1O_2$ quantum yield of 0.71.[14b] Interestingly, its chloride analogue $[\mathbf{5a}]^+$ only has a $^1O_2$ quantum yield of 0.023 under the same conditions, emphasizing the critical influence of the monodentate ligand on the photochemical and dioxygen photosensitizing properties of this family of complexes.

Cytotoxicity

The cytotoxic properties of the chloride complexes [**1a**]Cl–[**8a**]Cl and their caged analogues [**1b**]$(PF_6)_2$–[**8b**]$(PF_6)_2$ were evaluated against two different human cell lines: A549 (human lung carcinoma) and MCF-7 (human breast adenocarcinoma). Considering the photo-substitution properties of some of these complexes, their photocytotoxicity was also tested under blue light irradiation (3.2 ± 0.2 J cm^{-2} at 454 ± 11 nm), as described previously for [**5b**]$(PF_6)_2$.[14b] Cells were seeded at $t=0$, treated after 24 h with a concentration gradient of each ruthenium complex, irradiated or maintained in the dark after replacing the media, and further incubated in the dark for 48 h. At $t=96$ h cell viability was determined using the sulforhodamine B (SRB) assay.[24] The effective concentrations (EC_{50}), defined as the concentration at which a 50% survival rate on cell viability is observed, are reported in Table 3. Most chloride complexes were found to be non-cytotoxic, with the exception of [**8a**]Cl that was found moderately cytotoxic ($EC_{50}=28$ μM) against the MCF-7 cell line, in agreement with the value reported by Reedijk and co-workers.[25] The values for [**4a**]Cl (59 μM and 34 μM against A549 and MCF-7, respectively) were found similar to that observed for $[Ru(bpy)(dppz)_2]^{2+}$ analogues reported by the group of Schatzschneider.[26] Based on their results, it was expected that the structurally similar but more lipophilic dppn complex [**5a**]Cl would be cytotoxic, but no significant toxicity was observed for this complex. On the other hand, its EC_{50} could not be clearly determined due to the poor solubility of this complex in cell culture medium.[14b] Interestingly however, [**5a**]Cl was to be found cytotoxic upon blue light irradiation, with EC_{50} values of 9.7 and 3.2 μM for A549 and MCF-7 cells, respectively, corresponding to photoindexes (PI) of more than 2.6 and 7.9, respectively. This result is unexpected, because the $^1O_2$ quantum yield of [**5a**]Cl (0.023) is much lower than that of its glycoconjugated analogue [**5b**]$(PF_6)_2$ (0.71). A possible explanation would be the partial conversion, after uptake, of the chloride complex to its aquated counterpart $[Ru(tpy)(dppn)(H_2O)]^{2+}$ (Figure 4a), which has been demonstrated to be a good $^1O_2$ sensitizer (its close analogue $[Ru(toy)(dppn)(CD_3OD)]^{2+}$ has a $^1O_2$ production quantum yield under air of $\Phi_\Delta=0.43$).[14b] An alternative explanation would be that a different type of PDT is occurring, such as PDT type I, which is dependent upon the formation of radical species without intervention of molecular oxygen.[27] Further studies would be needed to conclude on the biological mechanism of the photocytotoxicity of [**5a**]Cl.

Table 3. Cytotoxicity of compounds [**1a**]Cl–[**8a**]Cl and [**1b**]$(PF_6)_2$–[**8b**]$(PF_6)_2$ towards A549 and MCF-7 cells in the dark and upon blue light irradiation (454 nm, 3.2 J cm^{-2}). Cell-growing inhibition effective concentrations (EC_{50}) are reported in μM with 95% confidence interval (CI) in μM. Data is the mean over three independent experiments. Photocytotoxicity index (PI) = $EC_{50dark}/EC_{50light}$ (dimensionless).

Complex[a]	Light dose [J cm^{-2}]	A549 EC_{50}	CI	PI	MCF-7 EC_{50}	CI	PI
[**1a**]Cl	0	>100		–	>100		–
	3.2	>100			>100		
[**2a**]Cl	0	>100		–	64	+12 −9.1	1.2
	3.2	>100			52	+15 −10	
[**3a**]Cl	0	>100		–	>100		–
	3.2	>100			>100		
[**4a**]Cl	0	59	+31 −21	1.3	34	+6.0 −5.1	1.1
	3.2	47	+19 −13		31	+4.8 −4.2	
[**5a**]Cl	0	>25		>2.6	>25		>7.9
	3.2	9.7	+4.4 −2.6		3.2	+1.3 −0.87	
[**6a**]Cl	0	>25		–	>25		–
	3.2	>25			>25		
[**7a**]Cl	0	>100		–	>100		–
	3.2	>100			>100		
[**8a**]Cl	0	>100		–	28	+4.9 −4.2	–
	3.2	–			–		
[**1b**]$(PF_6)_2$	0	>100		–	>100		–
	3.2	>100			>100		
[**2b**]$(PF_6)_2$	0	>100		–	>100		–
	3.2	>100			>100		
[**3b**]$(PF_6)_2$	0	>100		–	>100		–
	3.2	>100			>100		
[**4b**]$(PF_6)_2$	0	>100		–	>100		–
	3.2	>100			>100		
[**4b**]$(PF_6)_2$[c]	0	64	+17 −13	2.4	52	+12 −9.4	2.6
	3.2	27	+6.4 −5.2		20	+2.5 −2.2	
[**5b**]$(PF_6)_2$[d]	0	19	+4.0 −3.3	26	9.6	+2.9 −2.3	11
	3.2	0.72	+0.16 −0.13		0.86	+0.21 −0.17	
[**6b**]$(PF_6)_2$	0	>100		–	>100		–
	3.2	>100			>100		
[**7b**]$(PF_6)_2$	0	>100		–	>100		–
	3.2	>100			>100		
[**8b**]$(PF_6)_2$	0	>100		–	>100		–
	3.2	>100			>100		

[a] Standard protocol: Cells were incubated with compound for 24 h, followed by replacement of the media, kept in the dark, or irradiated with blue light (5 min at 454 nm, 10.5 mW cm^{-2}, 3.2 J cm^{-2}) and further incubated in the dark for 48 h. [b] As in standard protocol, but without replacing media during treatment (cells are irradiated in the presence of compound). [c] Ref. [14b].

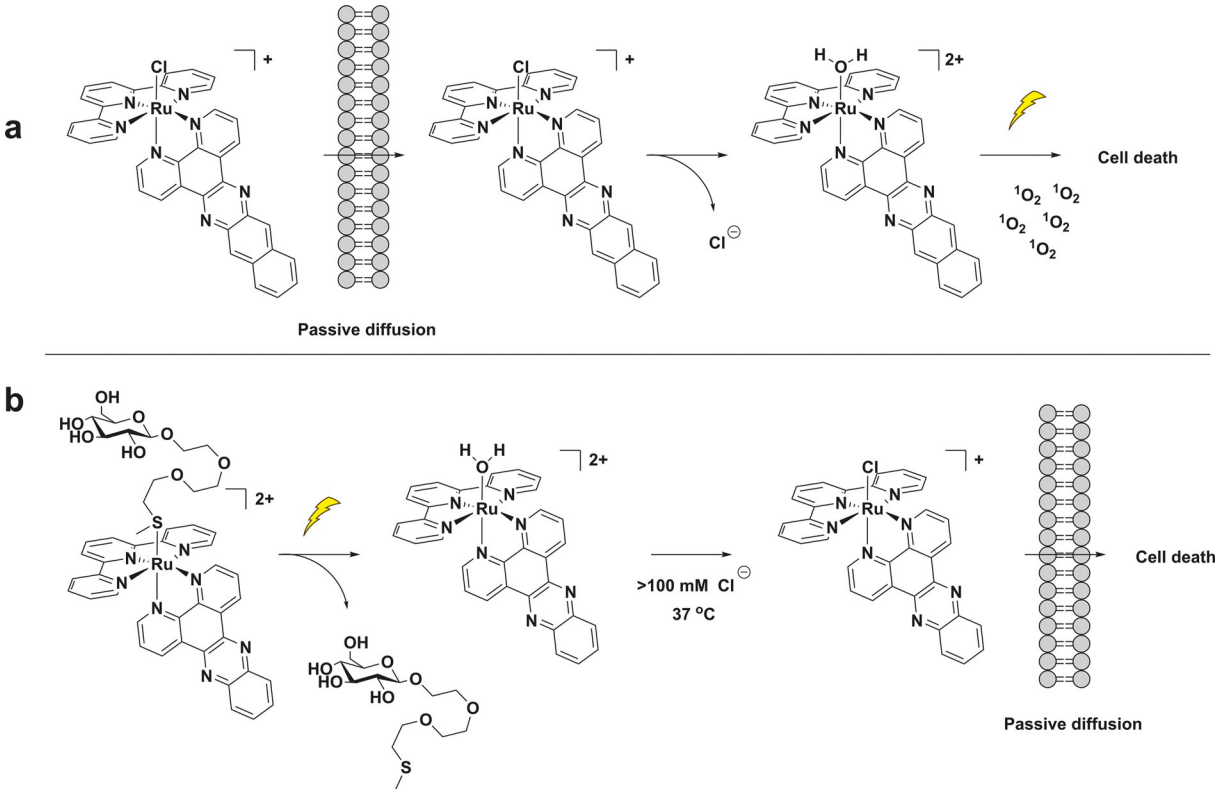

Figure 4. Proposed mechanisms for light-induced toxicity for a) [**5a**]Cl with media replacement, and b) [**4b**]$(PF_6)_2$ without media replacement. The lipid bilayer represents the cell membrane.

None of the glycoconjugated complexes were found to be photocytotoxic except [**5b**]$(PF_6)_2$, which was recently reported to enter passively into the cells and to destroy mitochondrial DNA by singlet oxygen generation.[14b] In our standard treatment protocol, media is replaced before light irradiation. In such conditions, photocytotoxicity can solely rely on the molecules that have been taken up by the cells during incubation, which may be a problem for highly hydrophilic glucose-conjugates such as [**1b**]$(PF_6)_2$–[**8b**]$(PF_6)_2$ (see below).

For compound [**4b**]$(PF_6)_2$, an adjustment of the protocol, consisting in irradiating the cells without media refreshing, led to a modest but clearly improved PI (2.4 and 2.6 for MCF-7 and A549, respectively). With such a protocol the full dose of compound added to each well remains present during and after irradiation, and most importantly activation may occur outside the cell, and be followed by cellular uptake of the activated photoproduct. For [**4b**]$(PF_6)_2$, the observed phototoxicity might thus be explained by the formation of the aquated species $[Ru(tpy)(dppz)(H_2O)]^{2+}$ outside the cell, followed by in situ conversion to the chloride species [**4a**]Cl due to the high chloride content in media (> 100 mM), followed by cellular uptake (Figure 4b). This interpretation is supported by the EC_{50} values found for [**4a**]Cl, which were not impressive but could clearly be measured (59 and 34 μM for A549 and MCF-7 respectively). Not refreshing the media before light activation did not lead to enhanced toxicity for [**1b**]$(PF_6)_2$–[**3b**]$(PF_6)_2$ and for [**6b**]$(PF_6)_2$–[**7b**]$(PF_6)_2$, showing that keeping high concentrations of the prodrug during and after light irradiation does not necessarily lead to enhanced phototoxicity. Overall, these results demonstrate that [**4b**]$(PF_6)_2$ is a moderately effective PACT agent,[3b] whereas the dppn analogues [**5a**]Cl and [**5b**]$(PF_6)_2$ are catalytic PDT sensitizers, which can be activated using a low dose of blue light. They also demonstrate that apparently minor differences in the treatment protocol of light-activated drugs may lead to very different interpretation of the cytotoxicity of light-activated compounds.

Log $P_{o/w}$ and uptake

To acquire more insight on the effect of glycoconjugation on the solubility, cellular uptake, and toxicity of these complexes, the water-octanol partition coefficients (log $P_{o/w}$) were determined for all complexes according to reported standards (Figure 5b).[28] As shown in Figure 5b (left), the chloride compounds with the smallest bidentate ligands, that is, [**1a**]Cl–[**3a**]Cl, have similar log $P_{o/w}$ values ranging from −0.81 to −1.1, while [**7a**]Cl and [**8a**]Cl have log $P_{o/w}$ values of −1.60 to −1.80. For these five complexes, the chloride counter anion provides appreciable water solubility. By contrast, the chloride compounds with the largest bidentate ligands, that is, [**4a**]Cl–[**6a**]Cl, are much more hydrophobic with log $P_{o/w}$ values ranging from −0.10 to +1.0. Although one may expect that the dicationic nature of [**1b**]$(PF_6)_2$–[**8b**]$(PF_6)_2$ and glycoconjugation should necessarily improve water solubility compared to their chloride analogues, we found that [**1b**]$(PF_6)_2$–[**3b**]$(PF_6)_2$ had similar log $P_{o/w}$ values (−0.11 to −0.51, respectively) compared

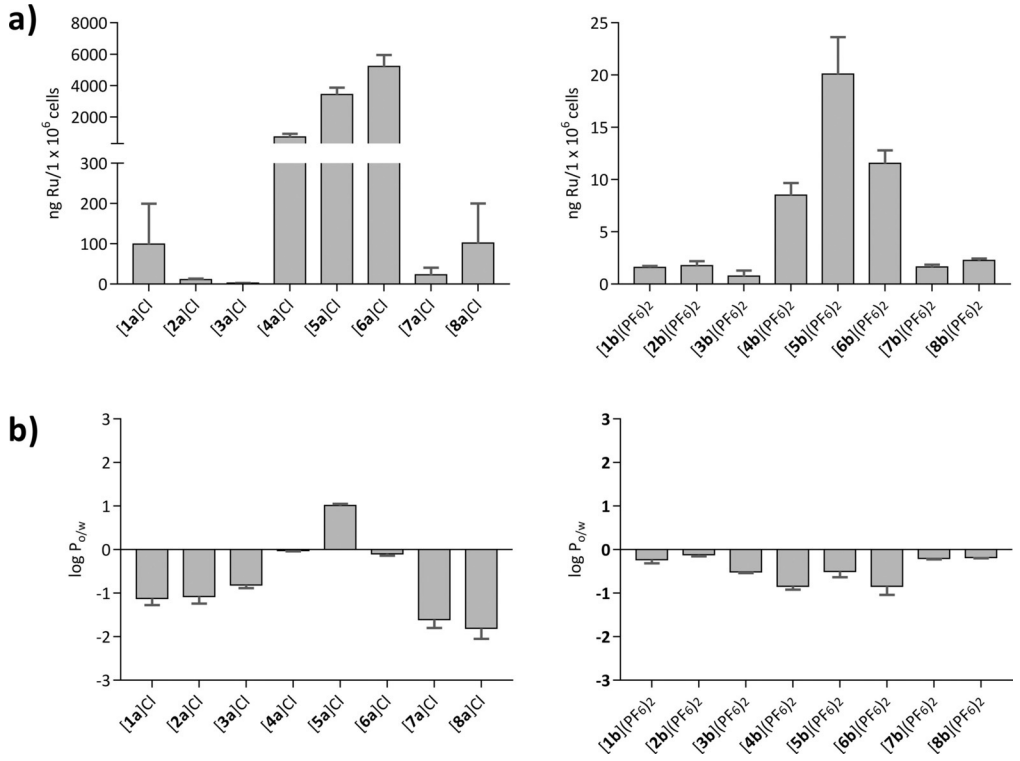

Figure 5. Intracellular uptake of 25 **μM** of [**1 a**]Cl–[**8 a**]Cl (left) and [**1 b**]-[**8 b**]$(PF_6)_2$ (right) in A549 cells after 24 h. Values are reported ± SD, $n = 2$. b) Log $P_{o/w}$ values found for [**1 a**]Cl--[**8 a**]Cl (left) and [**1 b**]$(PF_6)_2$–[**8 b**]$(PF_6)_2$ (right). Values are reported ±SD, $n = 3$.

to their analogues [**1 a**]Cl–[**3 a**]Cl, whereas [**7 b**]$(PF_6)_2$ and [**8 b**]$(PF_6)_2$ were slightly more hydrophobic (log $P_{o/w} = -0.20$ and −0.18, respectively) than [**7 a**]Cl and [**8 a**]Cl. This result points to the critical influence of the counterions, as the two hexafluoridophosphate anions of the glycoconjugate compounds increase lipophilicity, compared to chlorides. Furthermore, the chloride complexes are not stable in water, resulting in (partial) conversion to the $[Ru(tpy)(N–N)(H_2O)]Cl_2$ species which are more soluble in water than the hexafluoridophosphate salts of the **R**-substituted ruthenium complexes. The most hydrophobic chloride complexes [**4 a**]Cl–[**6 a**]Cl, that were much more difficult to dissolve in water, profited most from the glycoconjugation because [**4 b**]$(PF_6)_2$–[**6 b**]$(PF_6)_2$ indeed became water soluble (log $P_{o/w} = -0.84$ to −0.50, respectively). Overall glycoconjugation allowed for investigating the photochemistry of all thioether complexes [**1 b**]$(PF_6)_2$–[**8 b**]$(PF_6)_2$ in water.

To check whether the low toxicity of the thioether-glucose conjugates was not simply due to a low uptake, cellular uptake was studied for all sixteen complexes in A549 cells at a concentration of 25 μM, using an incubation time of 24 h and measuring intracellular ruthenium concentrations by ICP-MS. Although no general correlation could be found between the log $P_{o/w}$ values for these complexes and their cellular uptake, very strong differences in metal uptake were observed depending on the ligands and counterions (Figure 5 a). The most hydrophobic chloride compounds [**4 a**]Cl, [**5 a**]Cl and [**6 a**]Cl displayed very high metal uptake (> 1000 ng Ru per million cells), whereas their glycoconjugates [**4 b**]$(PF_6)_2$, [**5 b**]$(PF_6)_2$ and [**6 b**]$(PF_6)_2$ displayed cellular uptake that was much lower (10–20 ng Ru per million cells, for example, 250 times lower for [**5 b**]$(PF_6)_2$ compared to [**5 a**]Cl). Of course, this lower uptake can partially be explained by the lower log $P_{o/w}$ values of the glycoconjugates, and at least for [**5 b**]$(PF_6)_2$, by the absence of GLUT-based active uptake.[14b] However, [**4 b**]$(PF_6)_2$–[**6 b**]$(PF_6)_2$ are also taken up in 10-fold higher amounts than [**1 b**]$(PF_6)_2$–[**3 b**]$(PF_6)_2$, which have comparable log $P_{o/w}$ values. These results may not necessarily represent the conditions experienced by these compounds at the cell membrane, for which it is more likely that the lipophilic PF_6^- counterions are already exchanged for the more abundant and more water soluble chloride or phosphate anions in the buffer, canceling the effect of the PF_6^- anion on lipophilicity.

Discussion

Some of the chloride complexes [**1 a**]Cl–[**8 a**]Cl were thermally unstable and therefore no photodissociation quantum yields were determined, whereas their singlet oxygen properties were in general very low. The phototoxicity in the series of the most lipophilic compounds [**4 a**]Cl–[**6 a**]Cl cannot be explained by the trends observed in cell uptake and singlet oxygen generation. [**6 a**]Cl has indeed a higher singlet oxygen quantum yield (0.082) than [**4 a**]Cl and [**5 a**]Cl (0.005 and 0.023, respectively), but it is not phototoxic, whereas [**4 a**]Cl and [**5 a**]Cl are, and all three complexes are taken up in high amounts. In this series of complexes, different intracellular localization or biological targets, coupled to unknown photoreactions of [**5 a**]Cl,

must explain the differences in phototoxicity between [**6a**]Cl on the one hand and [**4a**]Cl and [**5a**]Cl on the other.

An opposite conclusion can be drawn for the glycoconjugates series [**4b**]$(PF_6)_2$, [**5b**]$(PF_6)_2$ and [**6b**]$(PF_6)_2$. The only phototoxic agent of this series, [**5b**]$(PF_6)_2$, has by far the highest singlet oxygen quantum yield (0.71 vs. 0.0010 and 0.0020), whereas all three compounds are taken up in similar amounts (10–20 ng Ru per million cell). Hence, [**5b**]$(PF_6)_2$ is at least an excellent PDT agent, whereas a PACT mode of action cannot be ruled out considering the phototoxic properties of [**5a**]Cl and its low singlet oxygen quantum yield. The phototoxicity observed for [**4b**]$(PF_6)_2$ when the protocol is slightly modified, suggests that this compound may act as a cytotoxic PACT agent. Furthermore [**4b**]$(PF_6)_2$ showed the highest photosubstitution quantum yield (0.02) and no significant singlet oxygen production. When cell-culture media was replaced before light irradiation, the glycoconjugate compound was not taken up in high amounts, and given the poor photodynamic properties of the photoproduct ($[\mathbf{4a}]^+$ or $[Ru(tpy)(dppz)(OH_2)]^{2+}$) not enough reactive oxygen species could be generated to kill the cells. This example demonstrates that the potential of [**4b**]$(PF_6)_2$ as a PACT agent is determined by the treatment protocol, which should be taken into account in further PACT studies. Furthermore, this complex has been shown to act has a DNA light-switch in the presence of DNA, which might be useful for theranostic applications.[29]

Conclusion

Overall eight chloride terpyridine complexes [**1a**]Cl–[**8a**]Cl with eight different bidendate spectator chelating ligands, and their eight thioether-glucose conjugates, were synthesized to compare the corresponding photophysical properties, photoreactivity, water solubility, cellular uptake, and phototoxicity. Depending on the bidentate ligand, these complexes can be considered either for photocaging, or for PACT and/or PDT. Compound [**8a**]Cl is not suitable for photocaging or phototherapy because the azo group of the azpy spectator ligand stabilizes the ^{3}MLCT states too much and prevents thermal population of the ^{3}MC state, thereby quenching photosubstitution. Singlet oxygen generation was also fully quenched in [**8a**]Cl and [**8b**]$(PF_6)_2$, emphasizing the poor photosensitizing properties of this compound. The five complexes [**1a**]Cl–[**3a**]Cl, [**6a**]Cl, and [**7a**]Cl, are non-toxic, and once substituted by thioethers, they form complexes with similar photosubstitution quantum yields ($\Phi_{450} \approx 0.01$) and low $^1O_2$ production quantum yields ($\Phi_\Delta < 0.10$). As a consequence, they are excellent candidates for the photocaging of thioether-based biologically active compounds, such as the antibiotics amoxicillin and clindamycin. The exceptionally high cellular uptake measured for [**6a**]Cl is worth noticing (5220 ± 737 ng Ru per million cells), considering that this compound did not show any measurable cytotoxicity at concentrations lower than 25 μM. It can even turn highly hydrophilic compounds such as R into species such as [**6b**]$(PF_6)_2$ that are still lipophilic enough to enter into cancer cells. Finally, [**4a**]Cl and [**5a**]Cl show similar lipophilicity compared to [**6a**]Cl and comparably high cellular uptake, but they also showed some toxicity both in the dark and after light activation. They are therefore less interesting as PACT carriers and instead have better potential as a either a cytotoxic PACT agent or for PDT, as we have recently demonstrated for [**5b**]$(PF_6)_2$.[14b] Overall, this work demonstrates that complexes based upon the $[Ru(tpy)(NN)(\mathbf{R})]^{n+}$ scaffold are good photocaging agents but poorly (photo)cytotoxic unless DNA intercalators such as dppz and dppn are chosen as a bidentate ligand, in which case they could serve as phototoxic agents.

Acknowledgements

This work was supportedby the Dutch Organization for Scientific Research (NWO-CW) with a VIDI grant to S.B. The European Research Council is kindly acknowledged for a Starting Grant to S.B. Prof. E. Bouwman is gratefully acknowledged for her support and input. Fons Lefeber and Dr. Karthick Sai Sankar Gupta are acknowledged for their help with NMR spectroscopy. Gerwin Spijksma is gratefully acknowledged for performing the HRMS measurements.

Conflict of interest

The authors declare no conflict of interest.

Keywords: cancer · light · photo-activated therapy (PACT) · photodynamic therapy (PDT) · ruthenium

[1] a) Z. Adhireksan, G. E. Davey, P. Campomanes, M. Groessl, C. M. Clavel, H. Yu, A. A. Nazarov, C. H. Yeo, W. H. Ang, P. Droge, U. Rothlisberger, P. J. Dyson, C. A. Davey, *Nat. Commun.* **2014**, *5*, 3462; b) M. H. Seelig, M. R. Berger, B. K. Keppler, *J. Cancer Res. Clin Oncol.* **1992**, *118*, 195–200; c) M. Colucci, M. Coluccia, P. Montemurro, M. Conese, A. Nassi, F. Loseto, E. Alessio, G. Mestroni, N. Semeraro, *Int. J. Oncol.* **1993**, *2*, 527–529; d) O. Novakova, J. Kasparkova, O. Vrana, P. M. Vanvliet, J. Reedijk, V. Brabec, *Biochemistry* **1995**, *34*, 12369–12378; e) A. C. G. Hotze, H. Kooijman, A. L. Spek, J. G. Haasnoot, J. Reedijk, *New J. Chem.* **2004**, *28*, 565–569.

[2] A.-M. Florea, D. Büsselberg, *Cancers* **2011**, *3*, 1351.

[3] a) S. Leijen, S. A. Burgers, P. Baas, D. Pluim, M. Tibben, E. van Werkhoven, E. Alessio, G. Sava, J. H. Beijnen, J. H. Schellens, *Invest. New Drugs* **2015**, *33*, 201–214; b) C. Mari, V. Pierroz, S. Ferrari, G. Gasser, *Chem. Sci.* **2015**, *6*, 2660–2686.

[4] G. Subramanian, P. Parakh, H. Prakash, *Photochem. Photobiol. Sci.* **2013**, *12*, 456–466.

[5] a) K. Davia, D. King, Y. L. Hong, S. Swavey, *Inorg. Chem. Commun.* **2008**, *11*, 584–586; b) F. Heinemann, J. Karges, G. Gasser, *Acc. Chem. Res.* **2017**, *50*, 2727–2736.

[6] J. Fong, K. Kasimova, Y. Arenas, P. Kaspler, S. Lazic, A. Mandel, L. Lilge, *Photochem. Photobiol. Sci.* **2015**, *14*, 2014–2023.

[7] L. M. Loftus, J. K. White, B. A. Albani, L. Kohler, J. J. Kodanko, R. P. Thummel, K. R. Dunbar, C. Turro, *Chem. Eur. J.* **2016**, *22*, 3704–3708.

[8] a) L. Zeng, P. Gupta, Y. Chen, E. Wang, L. Ji, H. Chao, Z. S. Chen, *Chem. Soc. Rev.* **2017**, *46*, 5771–5804; b) L. N. Lameijer, D. Ernst, S. L. Hopkins, M. S. Meijer, S. H. C. Askes, S. E. Le Devedec, S. Bonnet, *Angew. Chem. Int. Ed.* **2017**, *56*, 11549–11553.

[9] L. Zayat, C. Calero, P. Albores, L. Baraldo, R. Etchenique, *J. Am. Chem. Soc.* **2003**, *125*, 882–883.

[10] a) M. A. Sgambellone, A. David, R. N. Garner, K. R. Dunbar, C. Turro, *J. Am. Chem. Soc.* **2013**, *135*, 11274–11282; b) R. N. Garner, J. C. Gallucci, K. R. Dunbar, C. Turro, *Inorg. Chem.* **2011**, *50*, 9213–9215.

[11] T. Joshi, V. Pierroz, C. Mari, L. Gemperle, S. Ferrari, G. Gasser, *Angew. Chem. Int. Ed.* **2014**, *53*, 2960 – 2963; *Angew. Chem.* **2014**, *126*, 3004 – 3007.
[12] E. Wachter, D. K. Heidary, B. S. Howerton, S. Parkin, E. C. Glazer, *Chem. Commun.* **2012**, *48*, 9649 – 9651.
[13] a) M. K. Herroon, R. Sharma, E. Rajagurubandara, C. Turro, J. J. Kodanko, I. Podgorski, *Biol Chem.* **2016**, *397*, 571 – 582; b) A. Li, R. Yadav, J. K. White, M. K. Herroon, B. P. Callahan, I. Podgorski, C. Turro, E. E. Scott, J. J. Kodanko, *Chem. Commun.* **2017**, *53*, 3673 – 3676.
[14] a) V. H. S. van Rixel, B. Siewert, S. L. Hopkins, S. H. C. Askes, A. Busemann, M. A. Siegler, S. Bonnet, *Chem. Sci.* **2016**, *7*, 4922 – 4929; b) L. N. Lameijer, S. L. Hopkins, T. G. Breve, S. H. Askes, S. Bonnet, *Chem. Eur. J.* **2016**, *22*, 18484 – 18491.
[15] a) B. Siewert, V. H. van Rixel, E. J. van Rooden, S. L. Hopkins, M. J. Moester, F. Ariese, M. A. Siegler, S. Bonnet, *Chem. Eur. J.* **2016**, *22*, 10960 – 10968; b) R. E. Goldbach, I. Rodriguez-Garcia, J. H. van Lenthe, M. A. Siegler, S. Bonnet, *Chem. Eur. J.* **2011**, *17*, 9924 – 9929.
[16] A. Mijatovic, B. Smit, A. Rilak, B. Petrovic, D. Canovic, Z. D. Bugarcic, *Inorg. Chim. Acta* **2013**, *394*, 552 – 557.
[17] S. Bonnet, J. P. Collin, N. Gruber, J. P. Sauvage, E. R. Schofield, *Dalton Trans.* **2003**, 4654 – 4662.
[18] A. K. Mårtensson?, P. Lincoln, *Dalton Trans.* **2015**, *44*, 3604 – 3613.
[19] A. C. Hotze, J. A. Faiz, N. Mourtzis, G. I. Pascu, P. R. Webber, G. J. Clarkson, K. Yannakopoulou, Z. Pikramenou, M. J. Hannon, *Dalton Trans.* **2006**, 3025 – 3034.
[20] A. E. M. Boelrijk, A. M. J. Jorna, J. Reedijk, *J Mol Catal Chem.* **1995**, *103*, 73 – 85.
[21] A. Bahreman, B. Limburg, M. A. Siegler, E. Bouwman, S. Bonnet, *Inorg. Chem.* **2013**, *52*, 9456 – 9469.
[22] a) K. Hansongnern, U. Saeteaw, G. Mostafa, Y. C. Jiang, T. H. Lu, *Anal. Sci.* **2001**, *17*, 683 – 684; b) F. N. Rein, W. Chen, B. L. Scott, R. C. Rocha, *Acta Crystallogr. Sect. E* **2015**, *71*, 1017 – 1021.
[23] a) B. A. Albani, C. B. Durr, C. Turro, *J Phys Chem. A* **2013**, *117*, 13885 – 13892; b) J. D. Knoll, B. A. Albani, C. Turro, *Chem. Commun.* **2015**, *51*, 8777 – 8780.
[24] V. Vichai, K. Kirtikara, *Nat. Protoc.* **2006**, *1*, 1112 – 1116.
[25] E. Corral, A. C. Hotze, H. den Dulk, A. Leczkowska, A. Rodger, M. J. Hannon, J. Reedijk, *J. Biol. Inorg. Chem.* **2009**, *14*, 439 – 448.
[26] U. Schatzschneider, J. Niesel, I. Ott, R. Gust, H. Alborzinia, S. Wolfl, *ChemMedChem* **2008**, *3*, 1104 – 1109.
[27] A. P. Castano, T. N. Demidova, M. R. Hamblin, *Photodiagn. Photodyn. Ther.* **2004**, *1*, 279 – 293.
[28] OECD, Test No. 107: Partition Coefficient (*n*-octanol/water): Shake Flask Method, OECD Publishing, p. 4.
[29] M. Frasconi, Z. Liu, J. Lei, Y. Wu, E. Strekalova, D. Malin, M. W. Ambrogio, X. Chen, Y. Y. Botros, V. L. Cryns, J. P. Sauvage, J. F. Stoddart, *J. Am. Chem. Soc.* **2013**, *135*, 11603 – 11613.

Manuscript received: November 13, 2017
Accepted manuscript online: December 8, 2017
Version of record online: January 30, 2018

